HHS Public Access

Author manuscript

Invest Ophthalmol Vis Sci. Author manuscript; available in PMC 2016 July 26.

Published in final edited form as:

Invest Ophthalmol Vis Sci. 2007 September ; 48(9): 4050–4060. doi:10.1167/iovs.06-1216.

Morphological Characterization of Organized Extracellular Matrix Deposition by Ascorbic Acid-Stimulated Human Corneal Fibroblasts

Xiaoqing Guo[a], **Audrey E. K. Hutcheon**[a], **Suzanna A. Melotti**[b], **James D. Zieske**[a], **Vickery Trinkaus-Randall**[c], and **Jeffrey W. Ruberti**[a,b,*]

[a]Schepens Eye Research Institute and Department of Ophthalmology, Harvard Medical School, Boston, MA 02114, USA

[b]Department of Mechanical and Industrial Engineering, Northeastern University, Boston, MA 02115, USA

[c]Departments of Biochemistry and Ophthalmology, Boston University School of Medicine, Boston University, Boston, MA 02118

Abstract

Purpose—To characterize the structure and morphology of extracellular matrix (ECM) synthesized by untransformed, cultured human corneal fibroblasts in long-term cultures.

Methods—Human corneal stromal keratocytes were expanded in transwell culture in the presence of fetal bovine serum and a stable derivative of Vitamin C. The cells were allowed to synthesize a fibrillar ECM for up to five weeks. Constructs were assessed via light (phase contrast and differential interference contrast) and transmission (standard and quick freeze/deep etch) microscopy.

Results—Electron micrographs revealed stratified constructs with multiple parallel layers of cells and an extracellular matrix comprising parallel arrays of small, polydisperse fibrils (27–51 nm) which often alternate in direction. Differential interference contrast images demonstrated oriented ECM fibril arrays parallel to the plane of the construct while quick-freeze deep etch micrographs showed the details of the matrix interaction with fibroblasts via arrays of membrane surface structures.

Conclusions—Human keratocytes, cultured in a stable Vitamin C derivative, are capable of assembling extracellular matrix which comprise parallel arrays of ECM fibrils. The resulting constructs, which are highly cellular, exhibit morphology similar to the developing mammalian stroma where organized matrix is derived. The appearance of arrays of structures on the cell membranes suggest a role in the local organization of synthesized ECM. This model could provide critical insight into the fundamental processes which govern the genesis of organized connective tissues such as the cornea and may provide a scaffolding suitable for tissue-engineering a biomimetic stroma.

*Corresponding author: Jeffrey W. Ruberti, Ph.D.; Northeastern University, 360 Huntington Ave – 334 SN, Boston, MA, 02115 USA; Tel: 617-373-3984; Fax: 617-373-2921; j.ruberti@neu.edu.

INTRODUCTION

A fundamental characteristic of load-bearing collagenous tissue is the high-degree of anisotropy in the arrangement of the fibrils. This anisotropy is necessary if the tissue is to support significant loads as collagen fibrils are designed to transmit forces unidirectionally. Understanding how an *organized*, anisotropic collagenous matrix can arise from a population of synthetically active fibroblastic cells remains one of the most important basic science objectives associated with connective tissue research [1, 2]. Such an endeavor would also support efforts aimed at producing load-bearing constructs for tissue engineering. For the corneal stroma, which possesses exquisite organization on the nanoscale to allow transmission of incident light [3–5] and to resist intraocular pressure, the processes which direct matrix synthesis and organization are not well-understood.

During corneal development the collagen fibrils are assembled, aligned and arranged into lamellae of alternating orientation [6, 7]. How the cells exert control over the natural tendency of assembling collagen fibrils to form random arrays is a matter of conjecture. There appear to be two competing hypotheses concerning collagen fibril assembly: 1) that the fibroblastic cells form “surface crypts” within which procollagen is assembled into fibrils and “vectorially” discharged [8–10] and 2) that the fibroblasts work in concert to produce highly-concentrated monomer solutions which gain order through cholesteric effects [11, 12].

Studies describing the organizational changes as a function of time during development have been derived primarily from the study of the embryonic chick [7] or rabbit [6] cornea. These investigations, though instrumental to our understanding of the development of organized stromal matrix, suffer from limited temporal resolution. The development of an *in vitro* matrix synthesis model of corneal stromal development in a system that will allow direct observation could provide insight into how organized tissue is produced.

Tissue engineers have been developing culture systems for use as connective tissue replacements for almost two decades [13] (see early review (Langer and Vacanti 1993 [14]). Currently, the most successful tissue cultured *in vitro* is skin, which greatly enhanced the repertoire of tools available to the clinician [15]. The success of skin organotypic culture has stimulated tissue engineers to produce corneal constructs from the cells of a variety of different species including: rabbit, bovine, pig and human [16–21]. In general, the methods to produce these constructs are focused on the techniques necessary to successfully cultivate the cellular layers onto and within a randomly oriented self-assembled collagen-based gel. Tissue-engineered corneas produced in this way have lacked the mechanical strength and transparency required for clinical application [22]. However, a culture system which induces synthesis of an *in vivo*-like stromal matrix, could provide tissue engineers with a mechanically strong, transparent scaffolding onto which epithelial and endothelial layers could be seeded to produce a functional, organotypic cornea.

Although Vitamin C has been shown to increase the proliferative rate of cultured fibroblasts and stimulate the synthesis and secretion of appropriate ECM components,[23–27] it is not stable for long periods of time when exposed to culture conditions.[25, 28] In one investigation, primary human corneal fibroblasts were grown in short-term culture in the presence of

Vitamin C[29]. The fibroblasts produced heterotypic collagenous fibrils containing type I/V monomers and type VI collagen, which are present in normal human corneal stroma. Recently, more stable derivatives of ascorbic acid, L-ascorbic acid 2 phosphate (P-Asc) and 2-O-α-D-glucopyranosyl-L-ascorbic acid (G-Asc), collectively referred to as S-Asc (stabilized ascorbic acid), have been shown to enhance the synthesis and secretion of collagen by fibroblasts in culture [24–26, 30, 31].

In the current investigation, a new, long-term culture system comprising untransformed cultured human corneal fibroblasts was developed to induce the synthesis of an ECM *de novo* following stimulation with stabilized Vitamin C. Our system utilizes primary human corneal keratocytes which have been converted into fibroblasts by continual exposure to fetal bovine serum. The fibroblasts are then stimulated by S-Asc to synthesize and assemble a supportive ECM. The organization of the secreted extracellular matrix was characterized by light microscopy (phase and differential interference contrast (DIC)) and transmission electron microscopy (standard and quick freeze/deep etch (QFDE)). Indirect immunofluorescence was used to determine if type V or type VI collagen was synthesized.

MATERIAL AND METHODS

All procedures used in these studies adhered to the tenets of the Declaration of Helsinki. Human corneas were obtained from the National Disease Research Interchange (NDRI, Philadelphia, PA).

Primary culture of human corneal cells

Corneal epithelium and endothelium were removed from the stroma by scraping with a razor blade. The stromal tissue was cut into small pieces and put into 6-well plates (4 or 5 pieces of 2 × 2 mm tissue per well). Explants were allowed to adhere to the bottom of the wells at room temperature for 5 minutes before EMEM medium (Sigma-Aldrich; St. Louis, MO) containing 10% fetal bovine serum (FBS:ATCC; Manassas, Virginia) was added. Each 500 ml bottle of medium was supplemented with 5 ml of 1% antibiotic/antimycotic (Sigma). Care was taken when adding the medium to make sure that the explants remained attached to the wells. After 1–2 weeks cultivation (37°C, 5% CO_2), the fibroblasts were passaged into a T75 flask. The cells were grown to 100% confluency before their use in the culture system.

Fibroblast assembled extracellular matrix

The human corneal fibroblasts (HCFs) were plated on transwell 6-well plates with membrane inserts with 3.0 μm pores (Costar; Charlotte, NC) at a density of 0.5×10^6 cells/well. Membranes were either polyester or polycarbonate - qualitative comparisons of constructs demonstrated no difference between the surfaces. Fibroblasts were cultured in EMEM medium with 10% FBS and 1 mM L-Ascorbic Acid 2-Phosphate (P-Asc) or 0.5 mM 2-O-α-D-glucopyranosyl-L-ascorbic acid (G-Asc; Wako Chemicals USA, Inc.; Richmond, VA). As expected, preliminary investigations demonstrated that the use of either form of ascorbic acid produced similar results with regard to ECM production (thus data using either ascorbic acid was pooled). Medium was changed 3 times a week. The fibroblasts cultures were examined and imaged using phase contrast light microscopy [Zeiss Axiovert 25 (Carl

Zeiss MicroImaging, Inc.; Thornwood, NY) equipped with a Nikon D70 Digital Camera (Nikon Corporation; Tokyo, Japan)]. Except for a few constructs that were cryopreserved for QFDE electron microscopy at three and five weeks, the fibroblast cultures were allowed to generate constructs for 4 weeks. After 4 weeks in culture, the resulting constructs were processed using 1 or 2 of the following methods: (1) fixed in Karnovsky's fixative (2% paraformaldehyde, 2.5% gluteraldehyde in cacodylate buffer, pH 7.4) at 4°C for transmission electron microscopy (TEM); (2) frozen in O.C.T (Sakura; Torrance, CA) for indirect immunofluorescence microscopy; (3) slammed (rapidly frozen) for QFDE electron microscopy.

Light microscopy

The overall organization of the layering of the fibroblasts from day one to four weeks was monitored using phase contrast microscopy. The HCFs were viewed under phase illumination with an inverted microscope (Zeiss Axiovert 25) and imaged (Nikon D70 digital camera). Differential interference contrast imaging (DIC) of cultures was performed to estimate the total construct thickness and observe the orientation of synthesized fibrils relative to the HCF organization [32]. Constructs were gently removed from the underlying transwell membrane and placed in a drop of 1x phosphate buffered saline on a glass coverslip. A second coverslip was placed over the drop and construct and the whole preparation was placed on the stage of a Nikon TE2000U inverted microscope (Microvideo Instruments, Avon, MA). Z-scans were used to find the bottom and top of each construct to determine thickness. Within the Z-scans, images were taken to demonstrate the general alignment of the extracellular matrix in the plane of the construct.

Transmission electron microscopy (TEM)

The constructs were fixed overnight in Karnovsky fixative at 4°C and processed for TEM as described in Gipson et al. [33]. Briefly, constructs were fixed in strength Karnovsky's fixative, rinsed in PBS then processed through postfixation in 2% osmium tetroxide, en bloc staining in 0.5% uranyl acetate, alcohol dehydration to propylene oxide and embedded in Epon. Sixty nm sections cut transverse to the plane of the construct with a diamond knife ultramicrotome (LKB ultramicrotome; Bromma, Sweden) were viewed and photographed with a Philips 410 Transmission Electron Microscope (Philips Electronics N.V.; Eindhoven, The Netherlands).

Quick-Freeze/Deep Etch (QFDE)

A trephine was used to cut 3-mm specimens from the fibroblast constructs. These specimens, while still attached to the membrane, were rinsed with PBS to remove any excess medium then mounted tissue-side-up onto specimen carriers using a 2% Laponite solution (Rockwood Additives; Cheshire, UK) as an adhesive and cushioning material. After mounting the specimens, excess PBS was removed with filter paper, and the exposed surface of the tissue was rapidly slam frozen using a Leica EM CPC Cryoworkstation (Leica; Wetzlar, Germany). The frozen constructs were transferred into a Cressington CFE-60 freeze fracture/freeze etch system (Cressington Scientific Instrument; Watford, England) for replication. During replication, the specimens were superficially fractured and etched at −100°C for 25 min. Rotary shadowed replicas of the etched surfaces of the constructs were created by evaporation of platinum/carbon (for contrast) at 20° angle onto the rotating

construct, followed by evaporation of pure carbon (for replica strength) at a 90° angle. Tissue was digested overnight with household bleach. The cleaned replicas were picked up on copper 400-mesh grids. Grids were viewed and photographed with a Philips 410 Transmission Electron Microscope.

Fibril Diameter Estimation/cell volume percent estimation

Fibril diameter was estimated directly from the standard TEM images using calibration grids and Photoshop®; measurement tools. Fifty fibrils were selected randomly from multiple micrographs and were independent of position in the construct. For fibrils in cross-section, the smallest possible diametric line was chosen. For longitudinal fibrils, the thickest part of the fibril was measured. The data were reported as average ± standard deviation.

Cell volume as a percentage of the construct volume was estimated from low-magnification transmission electron micrographs from four different representative specimens. To perform the estimate, vertical lines were drawn from the top of the construct to the supporting membrane at three to four equally spaced points on each micrograph. The length of the line that intersected cellular material was divided by the total line length (construct thickness). The data were reported as average percent cellular volume ± standard deviation. It is well-known that standard TEM processing causes shrinkage in collagen and generally alters the volume of matrix and cells[34] and the data must be viewed with that caveat in mind.

Quantitative and Qualitative Demonstration of “Organization” in Constructs

Quantitative descriptions of “organization” can be obtained by demonstrating that features of the construct are “correlated” in some way. For instance, totally random arrays of collagen fibrils would not exhibit correlation in the angle of their long axes with any particular direction. To quantitatively demonstrate that our constructs possess an organized structure (i.e. different from a random structure) we examined transverse sections of TEM micrographs and measured the distribution of the angles of fibrils, cell bodies and cell processes which were parallel to the plane of the section. Fifteen random TEM micrographs were examined. Each micrograph was divided into a minimum of five regions. Within each region, the angle of longest continuous fibril (parallel to the plane of the section) was measured. The angles of the long axis of cells and cell processes in the cross-sections were also measured for comparison to the angles of the fibrils. The results of the examination are presented as average differences (and standard deviations) between the orientation angle of the cells and the synthesized collagen fibrils. Qualitatively, organization of the lamellae in the constructs was demonstrated by selecting micrographs where the collagen in the constructs clearly alternates in its alignment in adjacent lamellae. The presence of arrays of alternating structures, which cannot arise by random synthesis or self-assembly of collagen, should indicate that organizational control of fibrillogenesis is occurring in the cultures.

Collagen Type V and VI Indirect Immunofluorescence

Collagen type V is thought to play a role in the nucleation and control of collagen fibril diameter [35–39], and is found in significant quantities in normal human corneas. To detect type V collagen, fibrils in the construct were first partially disrupted in acetic acid [40]. Briefly, sections were washed in 0.1 M PBS three times each and incubated in 10 mM acetic

acid followed by two washes in PBS. The disrupted sections were fixed in 4% paraformaldehyde for 15 minutes and washed in PBS three times. The sections were blocked with 5% normal goat serum (NGS) in PBS, incubated in 1:200 mouse anti-collagen type V (Chemicon International, Temecula, CA) in PBS + NGS for two hours at room temperature. The sections were washed three times in PBS and incubated in 1:1000 goat anti-mouse Cy3 (Jackson ImmunoResearch, West Grove, PA) in PBS + NGS for 30 minutes at room temperature. Specimens were washed twice in PBS and coverslipped with mounting media containing DAPI, a marker for cell nuclei (Vectashield: Vector Laboratories; Burlingame, CA). Slides were viewed and imaged with a Nikon Eclipse E800 microscope equipped with a digital spot camera (MicroVideo Instruments, Avon, MA). Negative controls, where the primary antibody was omitted were performed.

Collagen type VI is a known component of the normal human corneal stroma [41]. To determine if our constructs were producing collagen type VI, immunoflourescence methods were employed. Specifically, sections were fixed in 4% paraformaldehyde for 15 minutes followed by three washes in PBS. The sections were transferred into 5% NGS in 0.1M PBS for 30 minutes and exposed for two hours to 1:200 rabbit anti-collagen type VI (Calbiochem, EMD Biosciences, Inc.; San Diego, CA) in PBS+NGS at room temperature. Sections were washed in PBS 3 times and incubated in goat anti-rabbit Cy3 (Jackson ImmunoResearch) in PBS+NGS for 30 minutes at room temperature. The sections were washed two times and viewed as described above.

RESULTS

Early culture cellular organization

After 1day, the HCFs formed a single layer of randomly oriented cells which exhibited a classic spindle-shape (Figure 1a). By 1 week, the culture had stratified into multiple layers where the long axes of fibroblasts exhibit orientation changes in different strata. The phase contrast micrograph (which constitutes an integrated Z-scan) of a one week old construct demonstrates the change in direction of the long axes of cells at different elevations above the transwell membrane. In some locations it appears that fibroblasts which are at the same x–y position but at different elevation have long axes which are oriented at approximately 90° angles to one another (Figure 1b). Our result confirms that of Newsome et al. [42] who showed similar behavior in human corneal fibroblasts.

Microscopic organization and morphology of mature cultures

By 4 weeks in culture, the HCFs stratified into multiple layers and produced significant quantities of ECM (Figure 2). The average construct total thickness at 4 weeks was 36.3±6.6 microns. Electron micrographs of the constructs in cross-section demonstrated that there were confluent monolayers of cells on the top of the culture as well as adjacent to the transwell (Figure 2). The presence of prominent rough endoplasmic reticulum indicates that the cells were synthetically active (Figure 5a).

The organization of the synthesized ECM, which was contained between bounding cellular monolayers, was similar to native corneal stroma in that arrays of fibrils often alternated in

direction (Figures 3a, 3b and 3c) and were parallel to both the transwell membrane and the cell body long axes (in the transverse plane). Quantitatively, the average difference in the measured angle between the cell axes and the transverse fibril orientation across all micrographs was 0.65° (± 0.49°; $n_{fibrils}$=90; n_{cells}=70). This demonstrates that in each construct the cells are aligned with the fibrils. If it is assumed that the transverse TEM sections were representative, then at all points in the construct, the fibrils and cell bodies may be considered parallel. Figure 3 shows TEM micrographs of representative HCF derived constructs which are *qualitatively* similar in organization to lamellae found in the normal cornea.

Nanoscale Collagen Organization/morphology

The fibril diameter determined from the micrographs was 38.1 ± 7.4 nm. However, the fibrils in the constructs were polydisperse in their diameter distribution (Figure 4a). Periodic banding can be seen on fibrils which were observed at higher resolution and in longitudinal section (Figure 4b). In addition to the larger fibrils, the constructs often exhibited clusters of microfibrils which have been observed in developing mammalian stromas[6, 7].

Cell Density and Cell-Fibril Apposition in cultures

It is important to note that the ratio of fibroblast-to-ECM volume was high (average cell volume: 45±9%) and that the general organization and a number of aspects of the HCF construct were strikingly similar to that of developing mammalian stroma [6]. Similarities include the close apposition of cells and cell processes (Figure 5a), the prominent rough endoplasmic reticulum RER (Figure 5a), the presence of clusters of microfibrils (Figure 4c), and the parallel alignment of fibrils adjacent to the cell membrane (Figure 5b).

DIC imaging of planar organization of aligned ECM in constructs

DIC imaging can be used to extract qualitative alignment information about the organization/alignment of extracellular matrix from cell cultures [32]. In our system, we used in plane DIC imaging to supplement the data obtained by the transverse TEM images (Figure 6). DIC imaging indicates that the constructs possess aligned structures (which we assume to be arrays of fibrils) which are parallel to each other over significant distances in the plane of the construct (Figure 6a). Because optical imaging possesses a diffraction limit, it is impossible to determine which structures contribute to the aligned “texture” in the micrograph. However, z-scan flythroughs of the constructs using DIC demonstrate alternating arrays of aligned structures (Figures 6b and 6c) consistent with the TEM images of fibrils in the constructs (Figure 3). Taken together, these data suggest qualitatively, that the constructs possess some degree of organization in their structure both transverse to and in the plane of the construct.

Details of cell/matrix interaction

Quick Freeze/Deep Etch images show that the HCFs in the constructs display areas of regularly spaced “indentations” on the fibroblast surface (Figure 7). Our interpretation is that the structures are *always* indentations into the cell. Protrusions are observed only when the fibroblast has been “torn” away from the membrane during fracture and we observe the

indentations from a perspective that is “inside the cell”. The images also demonstrate the presence of aligned small striated fibrils within a fairly dense fibrillar network (Figure 7b). Measurement of the fibrils found in the QFDE image (QFDE preserves fibril dimensions) demonstrated that the fibril diameters were small (approx 22 nm), polydisperse and that the diameter for individual fibrils varied along their axes. The size of these fibrils is not consistent with the diameter of the larger collagen fibrils found elsewhere in the culture by conventional TEM. However, the small diameter and density of fibrillar arrays is consistent with the weakly staining fibrillar structures found throughout the construct by conventional TEM (See Figure 9). Figure 7c shows a region of amazing regularity in the spacing of the surface indentations.

In Figure 8, the fracture plane has fortuitously revealed the intracellular matrix (ICM), the cell membrane (P-face) and the ECM. In addition, some details of the cell/matrix interaction are also elucidated. Within the ICM, it is possible to view the organization of the cell cytoskeleton which displays a significant degree of alignment. The images are *suggestive* that the cell cytoskeleton inserts into the membrane at the base of the indentations (Figure 8b) where it is possible to observe small, striated moieties (~15 nm in diameter). ECM fibrils, which are in close apposition with, and parallel to, the cell membrane appear to “dip” into the indentations on the cell surface. (Figure 8c).

The small size of the majority of the fibrils which were observed in the QFDE images might be explained by closer examination of the standard TEM images. Figure 9 shows a dense array of thin fibrils near a collagenous fibril which do not take up stain very well.

Collagen type V and VI in constructs

The constructs in this model were secreted by primary human fibroblasts stimulated with S-Asc. Under similar, but short-term culture conditions, HCFs have been shown to produce heterotypic type I/V fibrils and type VI collagen [29]. To ascertain whether our long-term cultures contained the collagens (other than type I) usually associated with human corneal stroma (type V and VI [41, 43]), immunofluorescence microscopy was employed. Collagen type V was detected throughout constructs following disruption of the fibrils by exposure to acetic acid (Figure 10a). Type V collagen appeared to stain some sections of the construct more heavily than other sections. Type VI collagen was found distributed throughout the construct (Figure 10b).

DISCUSSION

Microscopic Construct Organization

The corneal stroma is one of the most exquisitely organized ECMs in higher animals. Thus, working within the environment provided during stromal development, prospective corneal fibroblasts exert control over the natural tendency of collagen monomers to form randomly oriented fibrils [6, 7]. Retention of some of this ability to control collagen organization has been observed on a limited scale in three-dimensional culture systems [44, 45]. However, attempts to create engineered stromas by seeding degradable scaffoldings with relatively

diffuse concentrations of corneal fibroblasts have not resulted in the production of organized, mechanically strong, clear stromal ECM [17, 22].

Gaining a fundamental understanding of the mechanisms by which control over collagen fibrillogenesis is exerted could accelerate our ability to reproduce organized collagenous arrays on the benchtop and enhance our understanding of corneal fibrillogenesis. In the current study, our goal was to investigate whether untransformed donor human corneal fibroblasts, stimulated by a stabilized Vitamin C derivative in a scaffold-free system, can reaquire the ability to control collagen fibrillogenesis and assemble an ECM that is structurally similar to the human stroma (and not to scar tissue). The culture system may constitute a suitable model of stromal development (at least with regard to collagen synthesis) and should afford new opportunities to observe, with high spatial and temporal resolution, those mechanisms which control collagen fibrillogenesis and organization.

Previous studies [24–27] have shown that the addition of ascorbic acid can increase the proliferative rate of cultured fibroblasts and stimulate the synthesis and secretion of ECM components such as types I and type III collagen by acting as a cofactor for the enzymes responsible for hydroxylation of the lysine and proline residues on procollagen. This hydroxylation is required for the proper assembly of procollagen. Stabilized ascorbic acid (S-Asc, defined above), which extends the longevity of ascorbic acid in culture and has a potent effect on synthesis and secretion of ECM materials, can stimulate the stratification of dermal and corneal fibroblasts and has been shown to stimulate the production of ECM [46–4830.]

We have taken advantage of this effect to produce a corneal fibroblast-synthesized construct which begins with a single layer of cells in a scaffold-free system. Using the culture system supplemented with stabilized ascorbic acid, fibroblasts are shown to stratify to multiple layers, and have produced a collagenous ECM with organized, collagen fibril alignment, which alternates in adjacent “lamellae” within four weeks of seeding. We assume that the fibrils observed in our cultures are collagenous for the following reasons: 1) ascorbic-acid stimulated human corneal fibroblasts are known to produce type I/V heterotypic collagen fibrils under virtually identical culture conditions[29], 2) Normal corneal collagens (type V and VI) were detected in our cultures by immunofluorescence (see Figure 10) and 3) we are not aware of any striated fibrillar proteins of similar size that are not collagenous.

In many respects, the gross organization and architecture of the synthesized constructs was strikingly similar to that of a developing rabbit corneal stroma[6], including the high cell-to-matrix volume ratio, the presence of microfibrils, the prominent RER and the general parallel arrangement of the cells and adjacent ECM fibrils. The presence of the alternating layers of aligned collagen fibrils in “lamellae” produced by the HCFs suggests that those mechanisms which control collagen fibrillogenesis and organization are active in our culture system.

Fibril Diameter Distribution

With regard to the nanostructure of the fibrils themselves, it is important to examine fibril diameters. Corneal transparency depends on the local organization and composition of the

stromal ECM [49, 503, 4]. With regard to collagen, the spacing, fibril diameter and fibril polydispersity are important determinants of optical clarity (see recent review by Meek and Boote, 2004[51]). Examination of the standard TEM micrographs demonstrated that although organized arrays of aligned collagen fibrils were generated by the HCFs, the fibril diameters were generally larger and more polydisperse (38.1 ± 7.4 nm) than that found by investigators using similar means to image stromal collagen fibrils in adult humans (30.1 ± 2.5 [52]) and larger than those found in developing mammalian stromas (~30 nm[6]). For comparison purposes, highly-accurate x-ray synchrotron investigations place the fibril diameters in adult human corneas at 31 ± 0.8 nm [53]. The fact that the collagen fibrils in our system were larger and more polydisperse than those found in adult stroma may indicate that the ratio of collagens in the fibrils is not correct (type I/V heterotypic fibrils with a ratio of 4:1 [35, 54]) or possibly that other molecules which are thought to control fibril morphology such as proteoglycans are not present in appropriate concentrations [55–57]. It is important to note that our constructs, which were grown freely in a transwell without bounding membranes, are thus in a perpetually “swollen” state during growth. It is likely that some portion of secreted proteoglycans and other soluble molecules were able to diffuse into the medium where they could not influence the growing collagen fibrils [58].

Cell/Matrix Interaction

QFDE imaging, which has been used to study the fine structure of human, rabbit, chicken, bovine and developing avian corneal stroma [59–64], can reveal the interaction of the ECM with the cell membrane and cytoskeleton in exquisite detail. The images obtained via QFDE resulted in several observations of interest. The first is the presence of fine fibrils in an apparently very high density ECM, which are “sandwiched” between the fibroblasts (Figure 7a). The fibrils and microfibrils observed in the QFDE image do not appear to correspond well with the apparent sparsity and fibril size in the collageneous matrix observed in the standard TEM images (Figure 5a). This is not surprising as it is well-known that QFDE imaging captures more structural information than standard TEM because it does not rely on stains to absorb electrons and because there is no dehydration step. Instead, any structure that can be coated with platinum is replicated. On closer inspection of the ECM in standard TEM images however, we do observe a dense matrix of fine fibrils that do not appear to take up the stain very well (Figure 9). Weakly staining fibrils of similar size have been observed in developing rabbit stroma as well [6].

QFDE imaging also revealed the presence of arrays of shallow indentations on the surface of cells, which in some cases are extremely regular in their arrangement (Figure 7c). Though arrays of similarly-sized indentations on adult human *corneal keratocytes* in explants have been observed previously [65], their presence in our cultures of corneal fibroblasts was not expected. The size of these indentations is also consistent with that of caveolae found in some fibroblasts (for review see Anderson[66]). However, their morphological structure and apparent interaction is not consistent with caveolae[66]. Figure 8a suggests that the indentations comprise a network of “binding” sites for fibrils in the ECM, which appear to run parallel to the membrane surface. Though this is clearly speculative, the presence of the indentations in organized arrays and the apparent binding of the indentations to fibrils in the ECM are *suggestive* of a role in the control of matrix organization.

The fortuitous fracture of the fibroblast cytoskeleton in Figure 8a suggests that the arrays of indentations are also coupled to the cytoplasmic matrix. The details of the molecular linkage to the cytoskeleton cannot be extracted from the QFDE images without performing extensive immunolabelling combined with further QFDE imaging. However, it is quite possible that the indentations and their coupling molecules comprise a complex ECM attachment system for the fibroblasts [67].

Synthesizing Organized Matrix – Fibripositors and Cholesteric Control

The synthesis of organized collagenous matrix by S-Asc stimulated HCFs is certainly not a perfect analog for stromal development. Nonetheless, the fact that they are capable of producing significant quantities of aligned collagenous fibrils, packed into arrays which alternate in direction is a *de facto* proof that the cells in our model have significant control over matrix organization. In our system, we are evaluating two prevailing theories that explain the deposition of organized collagen by fibroblasts. The first theory was developed primarily in studies on tendon morphogenesis and proposes that fibroblast cells form tubular invaginations or “surface crypts” in their membranes where collagen monomers are confined and induced to form fibrils which have a particular orientation [8]. The fibrils are subsequently “vectorially discharged” from these putative “fibripositors” [68, 69] into the open extracellular space. Precisely how the cells then “stitch” together an organized matrix is not obvious. It is clear that for the fibropositor model to be correct in the cornea, there must be an organized migration of cells coupled with end-to-end fibril fusion such that the discharged fibrils are laid down in the correct orientation and over the correct distance. That fibroblasts migrate in the direction of aligned features (contact guidance [70]) or along lines of elevated strain or rigidity (durotaxis [71]) has been established experimentally. However, our culture system possesses no preferred orientation, contact guidance features or regions of enhanced substrate rigidity to cue the cells. Thus in our constructs, the fibropositor theory would require that the cells move in different directions in adjacent lamellae.

The second theory postulates that collagen monomers are secreted into the extracellular space in great enough concentration that they become “cholesterically” organized into patterns which reflect the local geometry [72, 73]. In the developing cornea[6, 74] and in our constructs, there is a high cell-to-matrix volume ratio and the cells are aligned and parallel to one another. The cholesteric control of collagen fibrillogenesis theory does not require orchestrated cell movement, just a high cell density and high collagen concentration. The relatively small space between cells, the appearance of highly-organized collagen within that confined space (which contains a dense ECM) and the extremely dense matrix shown by QFDE is consistent with the theory of cholesteric control of matrix organization. The alternating orientation of collagen fibrils in adjacent lamellae, both in our constructs and in developing stroma, is difficult to explain unless the cell surface is capable of influencing the forming fibril orientation. DIC imaging of the confluent monolayer of cells on the transwell membrane suggest that secreted collagen does indeed align along the long axis of spindle shaped fibroblasts[75]. The natural tendency of fibroblasts to change orientation in adjacent confluent layers could explain the alternating collagen orientation if the collagen does align with the body of the cells.

Conclusions

This is the first investigation to demonstrate that untransformed human corneal fibroblasts in a scaffold-free system can produce a *substantial,* organized, three-dimensional matrix that bears qualitative resemblance to the architecture of a developing mammalian corneal stroma[6]. It is our opinion that to produce such organized matrix, it is important that the culture system mimic *development*, where organized matrix is readily and rapidly produced. As in development, we begin with a high density of fibroblastic cells and with no provisional matrix or scaffolding. Using this approach, the fibroblasts, which are in close proximity, appear to effectively control the local organization of the matrix that they produce. Development is decidedly different from scar resolution which begins with a provisional matrix or scaffold that is remodeled over long periods of time[76, 77]. Recent attempts to produce engineered corneas mimic stromal scar resolution and begin by seeding fibroblasts at low density into degradable scaffoldings[16, 17, 22]. The resulting matrix, which is intended to replace the disorganized degrading scaffolding, does not exhibit organized arrays of collagen fibrils[78].

Though our model is not a perfect analog for stromal development, there are some strong similarities, which suggest that the same mechanisms may be involved in the syntheses of the organized arrays of collagen fibrils. It is therefore a potentially powerful tool in which to study how fibroblasts produce organized matrix. Investigation of this process could lead to better methods to produce organized tissue replacements *de novo*.

The organized matrix produced by this scaffold-free system could also provide a suitable starting point for artificial stroma. It is already possible to stack multiple constructs to produce a full thickness “stromal analog”. However the complex microarchitecture of a native cornea could not be easily reproduced in this manner[79, 80]. Other components of the developmental environment must be reproduced to refine the matrix morphology, such as application of *in vivo* loads[81] and/or co-culture with other cell populations[21, 82].

Acknowledgments

This investigation was supported by NIH/NEI 1R01 EY015500-01. The authors would like to thank Pat Pearson for her excellent transmission electron microscopy work and Tatfong Ng for the collagen staining and microscopy. We also appreciate the help of Professor David Birk for many insightful discussions on collagen and ECM structure.

References

1. Cowin SC. How is a tissue built? J Biomech Eng. 2000; 122:553–69. [PubMed: 11192375]
2. Cowin SC. Tissue growth and remodeling. Annu Rev Biomed Eng. 2004; 6:77–107. [PubMed: 15255763]
3. Goldman JN, Benedek GB. The relationship between morphology and transparency in the nonswelling corneal stroma of the shark. Invest Ophthalmol. 1967; 6:574–600. [PubMed: 6073962]
4. Hart RW, Farrell RA. Light scattering in the cornea. J Opt Soc Am. 1969; 59:766–774. [PubMed: 5805456]
5. Cox JL, Farrell RA, Hart RW, Langham ME. The transparency of the mammalian cornea. J Physiol. 1970; 210:601–16. [PubMed: 5499815]
6. Cintron C, Covington H, Kublin CL. Morphogenesis of rabbit corneal stroma. Invest Ophthalmol Vis Sci. 1983; 24:543–56. [PubMed: 6841000]
7. Hay, ED.; Revel, JP. Fine structure of the developing avian cornea. New York: Basel; 1969.

8. Birk DE, Trelstad RL. Fibroblasts create compartments in the extracellular space where collagen polymerizes into fibrils and fibrils associate into bundles. Annals of the New York Academy of Sciences. 1985; 460:258–66. [PubMed: 3868950]
9. Kadler KE, Holmes DF, Trotter JA, Chapman JA. Collagen fibril formation. Biochem J. 1996; 316(Pt 1):1–11. [PubMed: 8645190]
10. Hay, ED. Cell Biology of the Extracellular Matrix. 2. Hay, ED., editor. New York: Plenum Press; 1991. p. 468
11. Giraud-Guille MM. Twisted liquid crystalline supramolecular arrangements in morphogenesis. Int Rev Cytol. 1996; 166:59–101. [PubMed: 8881773]
12. Giraud-Guille MM, Besseau L, Martin R. Liquid crystalline assemblies of collagen in bone and in vitro systems. J Biomech. 2003; 36:1571–9. [PubMed: 14499304]
13. Matsuda T, Akutsu T, Kira K, Matsumoto H. Development of hybrid compliant graft: rapid preparative method for reconstruction of a vascular wall. ASAIO Trans. 1989; 35:553–5. [PubMed: 2597532]
14. Langer R, Vacanti JP. Tissue engineering. Science. 1993; 260:920–6. [PubMed: 8493529]
15. Beele H. Artificial skin: past, present and future. Int J Artif Organs. 2002; 25:163–73. [PubMed: 11999188]
16. Germain L, Auger FA, Grandbois E, et al. Reconstructed human cornea produced in vitro by tissue engineering. Pathobiology. 1999; 67:140–7. [PubMed: 10394135]
17. Griffith M, Osborne R, Munger R, et al. Functional human corneal equivalents constructed from cell lines. Science. 1999; 286:2169–72. [PubMed: 10591651]
18. Minami Y, Sugihara H, Oono S. Reconstruction of cornea in three-dimensional collagen gel matrix culture. Invest Ophthalmol Vis Sci. 1993; 34:2316–24. [PubMed: 7685009]
19. Orwin EJ, Hubel A. In vitro culture characteristics of corneal epithelial, endothelial, and keratocyte cells in a native collagen matrix. Tissue Eng. 2000; 6:307–19. [PubMed: 10992428]
20. Schneider AI, Maier-Reif K, Graeve T. Constructing an in vitro cornea from cultures of the three specific corneal cell types. In Vitro Cell Dev Biol Anim. 1999; 35:515–26. [PubMed: 10548433]
21. Zieske JD, Mason VS, Wasson ME, et al. Basement membrane assembly and differentiation of cultured corneal cells: importance of culture environment and endothelial cell interaction. Exp Cell Res. 1994; 214:621–33. [PubMed: 7523155]
22. Orwin EJ, Borene ML, Hubel A. Biomechanical and optical characteristics of a corneal stromal equivalent. J Biomech Eng. 2003; 125:439–44. [PubMed: 12968568]
23. Russell SB, Russell JD, Trupin KM. Collagen synthesis in human fibroblasts: effects of ascorbic acid and regulation by hydrocortisone. J Cell Physiol. 1981; 109:121–31. [PubMed: 7328129]
24. Pasonen-Seppanen S, Suhonen TM, Kirjavainen M, et al. Vitamin C enhances differentiation of a continuous keratinocyte cell line (REK) into epidermis with normal stratum corneum ultrastructure and functional permeability barrier. Histochem Cell Biol. 2001; 116:287–97. [PubMed: 11702187]
25. Hata R, Senoo H. L-ascorbic acid 2-phosphate stimulates collagen accumulation, cell proliferation, and formation of a three-dimensional tissuelike substance by skin fibroblasts. J Cell Physiol. 1989; 138:8–16. [PubMed: 2910890]
26. Nusgens BV, Humbert P, Rougier A, et al. Topically applied vitamin C enhances the mRNA level of collagens I and III, their processing enzymes and tissue inhibitor of matrix metalloproteinase 1 in the human dermis. J Invest Dermatol. 2001; 116:853–9. [PubMed: 11407971]
27. Saika S, Uenoyama K, Hiroi K, Ooshima A. L-ascorbic acid 2-phosphate enhances the production of type I and type III collagen peptides in cultured rabbit keratocytes. Ophthalmic Res. 1992; 24:68–72. [PubMed: 1608599]
28. Bergethon PR, Mogayzel PJ Jr, Franzblau C. Effect of the reducing environment on the accumulation of elastin and collagen in cultured smooth-muscle cells. Biochem J. 1989; 258:279–84. [PubMed: 2930513]
29. Ruggiero F, Burillon C, Garrone R. Human corneal fibrillogenesis. Collagen V structural analysis and fibrillar assembly by stromal fibroblasts in culture. Invest Ophthalmol Vis Sci. 1996; 37:1749–60. [PubMed: 8759342]

30. Kumano Y, Sakamoto T, Egawa M, Tanaka M, Yamamoto I. Enhancing effect of 2-O-alpha-D-glucopyranosyl-L-ascorbic acid, a stable ascorbic acid derivative, on collagen synthesis. Biol Pharm Bull. 1998; 21:662–6. [PubMed: 9703245]
31. Saika S. Ultrastructural effect of L-ascorbic acid 2-phosphate on cultured keratocytes. Cornea. 1992; 11:439–45. [PubMed: 1424673]
32. Petroll WM, Ma L. Direct, dynamic assessment of cell-matrix interactions inside fibrillar collagen lattices. Cell Motil Cytoskeleton. 2003; 55:254–64. [PubMed: 12845599]
33. Gipson IK, Grill SM, Spurr SJ, Brennan SJ. Hemidesmosome formation in vitro. J Cell Biol. 1983; 97:849–57. [PubMed: 6885921]
34. Craig AS, Robertson JG, Parry DA. Preservation of corneal collagen fibril structure using low-temperature procedures for electron microscopy. J Ultrastruct Mol Struct Res. 1986; 96:172–5. [PubMed: 3119734]
35. Birk DE, Fitch JM, Babiarz JP, Doane KJ, Linsenmayer TF. Collagen fibrillogenesis in vitro: interaction of types I and V collagen regulates fibril diameter. J Cell Sci. 1990; 95(Pt 4):649–57. [PubMed: 2384532]
36. Birk DE, Fitch JM, Babiarz JP, Linsenmayer TF. Collagen type I and type V are present in the same fibril in the avian corneal stroma. J Cell Biol. 1988; 106:999–1008. [PubMed: 3346334]
37. McLaughlin JS, Linsenmayer TF, Birk DE. Type V collagen synthesis and deposition by chicken embryo corneal fibroblasts in vitro. J Cell Sci. 1989; 94(Pt 2):371–9. [PubMed: 2621231]
38. Wenstrup RJ, Florer JB, Brunskill EW, Bell SM, Chervoneva I, Birk DE. Type V collagen controls the initiation of collagen fibril assembly. J Biol Chem. 2004; 279:53331–7. [PubMed: 15383546]
39. White J, Werkmeister JA, Ramshaw JA, Birk DE. Organization of fibrillar collagen in the human and bovine cornea: collagen types V and III. Connect Tissue Res. 1997; 36:165–74. [PubMed: 9512886]
40. Linsenmayer TF, Fitch JM, Schmid TM, et al. Monoclonal antibodies against chicken type V collagen: production, specificity, and use for immunocytochemical localization in embryonic cornea and other organs. J Cell Biol. 1983; 96:124–32. [PubMed: 6186670]
41. Zimmermann DR, Trueb B, Winterhalter KH, Witmer R, Fischer RW. Type VI collagen is a major component of the human cornea. FEBS Lett. 1986; 197:55–8. [PubMed: 3512309]
42. Newsome DA, Takasugi M, Kenyon KR, Stark WF, Opelz G. Human corneal cells in vitro: morphology and histocompatibility (HL-A) antigens of pure cell populations. Invest Ophthalmol. 1974; 13:23–32. [PubMed: 4588560]
43. Konomi H, Hayashi T, Nakayasu K, Arima M. Localization of type V collagen and type IV collagen in human cornea, lung, and skin. Immunohistochemical evidence by anti-collagen antibodies characterized by immunoelectroblotting. Am J Pathol. 1984; 116:417–26. [PubMed: 6383060]
44. Doane KJ, Babiarz JP, Fitch JM, Linsenmayer TF, Birk DE. Collagen fibril assembly by corneal fibroblasts in three-dimensional collagen gel cultures: small-diameter heterotypic fibrils are deposited in the absence of keratan sulfate proteoglycan. Exp Cell Res. 1992; 202:113–24. [PubMed: 1511726]
45. Doane KJ, Birk DE. Fibroblasts retain their tissue phenotype when grown in three-dimensional collagen gels. Exp Cell Res. 1991; 195:432–42. [PubMed: 2070825]
46. Germain L, Carrier P, Auger FA, Salesse C, Guerin SL. Can we produce a human corneal equivalent by tissue engineering? Prog Retin Eye Res. 2000; 19:497–527. [PubMed: 10925241]
47. Germain L, Remy-Zolghadri M, Auger F. Tissue engineering of the vascular system: from capillaries to larger blood vessels. Med Biol Eng Comput. 2000; 38:232–40. [PubMed: 10829419]
48. Michel M, L'Heureux N, Pouliot R, Xu W, Auger FA, Germain L. Characterization of a new tissue-engineered human skin equivalent with hair. In Vitro Cell Dev Biol Anim. 1999; 35:318–26. [PubMed: 10476918]
49. Maurice DM. The structure and transparency of the cornea. Journal of Physiology. 1957; 136:263–286. [PubMed: 13429485]
50. Benedek GB. Theory of the transparency of the eye. Applied Optics. 1971; 10:459–473. [PubMed: 20094474]

51. Meek KM, Boote C. The organization of collagen in the corneal stroma. Exp Eye Res. 2004; 78:503–12. [PubMed: 15106929]
52. Freund DE, McCally RL, Farrell RA, Cristol SM, L'Hernault NL, Edelhauser HF. Ultrastructure in anterior and posterior stroma of perfused human and rabbit corneas. Relation to transparency. Invest Ophthalmol Vis Sci. 1995; 36:1508–23. [PubMed: 7601631]
53. Meek KM, Leonard DW. Ultrastructure of the corneal stroma: a comparative study. Biophys J. 1993; 64:273–80. [PubMed: 8431547]
54. Birk DE. Type V collagen: heterotypic type I/V collagen interactions in the regulation of fibril assembly. Micron. 2001; 32:223–37. [PubMed: 11006503]
55. Brown CT, Lin P, Walsh MT, Gantz D, Nugent MA, Trinkaus-Randall V. Extraction and purification of decorin from corneal stroma retain structure and biological activity. Protein Expr Purif. 2002; 25:389–99. [PubMed: 12182818]
56. Chakravarti S, Magnuson T, Lass JH, Jepsen KJ, LaMantia C, Carroll H. Lumican regulates collagen fibril assembly: skin fragility and corneal opacity in the absence of lumican. J Cell Biol. 1998; 141:1277–86. [PubMed: 9606218]
57. Chakravarti S, Zhang G, Chervoneva I, Roberts L, Birk DE. Collagen fibril assembly during postnatal development and dysfunctional regulation in the lumican-deficient murine cornea. Dev Dyn. 2006; 235:2493–506. [PubMed: 16786597]
58. Kangas TA, Edelhauser HF, Twining SS, O'Brien WJ. Loss of stromal glycosaminoglycans during corneal edema. Invest Ophthalmol Vis Sci. 1990; 31:1994–2002. [PubMed: 2210995]
59. Barge A, Ruggiero F, Garrone R. Structure of the basement membrane of corneal epithelium: quick-freeze, deep-etch comparative study of networks deposited in culture and during development. Biol Cell. 1991; 72:141–7. [PubMed: 1756303]
60. Hirsch M, Nicolas G, Poulinquen Y. Interfibrillar structures in fast-frozen, deep-etched and rotary-shadowed extraceullar matrix of the rabbit corenal stroma. Experimental Eye Research. 1989; 49:311–315. [PubMed: 2767179]
61. Hirsch M, Noske W, Prenant G, Renard G. Fine structure of the developing avian corneal stroma as revealed by quick-freeze, deep-etch electron microscopy. Exp Eye Res. 1999; 69:267–77. [PubMed: 10471335]
62. Hirsch M, Prenant G, Renard G. Three-dimensional supramolecular organization of the extracellular matrix in human and rabbit corneal stroma, as revealed by ultrarapid-freezing and deep-etching methods. Exp Eye Res. 2001; 72:123–35. [PubMed: 11161728]
63. Overby D, Ruberti J, Gong H, Freddo TF, Johnson M. Specific hydraulic conductivity of corneal stroma as seen by quick-freeze/deep-etch. J Biomech Eng. 2001; 123:154–61. [PubMed: 11340876]
64. Yamabayashi S, Ohno S, Aguilar RN, Furuya T, Hosoda M, Tsukahara S. Ultrastructural studies of collagen fibers of the cornea and sclera by a quick-freezing and deep-etching method. Ophthalmic Res. 1991; 23:320–9. [PubMed: 1803313]
65. Muller LJ, Pels L, Vrensen GF. Novel aspects of the ultrastructural organization of human corneal keratocytes. Invest Ophthalmol Vis Sci. 1995; 36:2557–67. [PubMed: 7499078]
66. Anderson RG. The caveolae membrane system. Annu Rev Biochem. 1998; 67:199–225. [PubMed: 9759488]
67. Petroll WM, Ma L, Jester JV. Direct correlation of collagen matrix deformation with focal adhesion dynamics in living corneal fibroblasts. J Cell Sci. 2003; 116:1481–91. [PubMed: 12640033]
68. Canty EG, Kadler KE. Procollagen trafficking, processing and fibrillogenesis. J Cell Sci. 2005; 118:1341–53. [PubMed: 15788652]
69. Canty EG, Lu Y, Meadows RS, Shaw MK, Holmes DF, Kadler KE. Coalignment of plasma membrane channels and protrusions (fibripositors) specifies the parallelism of tendon. J Cell Biol. 2004; 165:553–63. [PubMed: 15159420]
70. Guido S, Tranquillo RT. A methodology for the systematic and quantitative study of cell contact guidance in oriented collagen gels. Correlation of fibroblast orientation and gel birefringence. J Cell Sci. 1993; 105(Pt 2):317–31. [PubMed: 8408268]

71. Lo CM, Wang HB, Dembo M, Wang YL. Cell movement is guided by the rigidity of the substrate. Biophys J. 2000; 79:144–52. [PubMed: 10866943]

72. Giraud-Guille MM, Besseau L. Banded patterns in liquid crystalline phases of type I collagen: relationship with crimp morphology in connective tissue architecture. Connect Tissue Res. 1998; 37:183–93. [PubMed: 9862220]

73. Giraud-Guille MM. Liquid crystallinity in condensed type I collagen solutions. A clue to the packing of collagen in extracellular matrices. J Mol Biol. 1992; 224:861–73. [PubMed: 1569562]

74. Sevel D, Isaacs R. A re-evaluation of corneal development. Trans Am Ophthalmol Soc. 1988; 86:178–207. [PubMed: 2979018]

75. Zieske, J.; Guo, X.; Melotti, S.; Hutcheon, A.; Ruberti, J. Spatial organization of engineered corneal stroma: Is there a need for contact guidance or direct mechanical stimulus?. 5th World Congress of Biomechanics; 2006; Munich, Germany.

76. Cintron C, Hong BS, Kublin CL. Quantitative analysis of collagen from normal developing corneas and corneal scars. Curr Eye Res. 1981; 1:1–8. [PubMed: 7297090]

77. Cintron C, Szamier RB, Hassinger LC, Kublin CL. Scanning electron microscopy of rabbit corneal scars. Invest Ophthalmol Vis Sci. 1982; 23:50–63. [PubMed: 7085221]

78. Crabb RA, Chau EP, Decoteau DM, Hubel A. Microstructural characteristics of extracellular matrix produced by stromal fibroblasts. Ann Biomed Eng. 2006; 34:1615–27. [PubMed: 17016762]

79. Radner W, Mallinger R. Interlacing of collagen lamellae in the midstroma of the human cornea. Cornea. 2002; 21:598–601. [PubMed: 12131038]

80. Radner W, Zehetmayer M, Aufreiter R, Mallinger R. Interlacing and cross-angle distribution of collagen lamellae in the human cornea. Cornea. 1998; 17:537–43. [PubMed: 9756449]

81. Altman GH, Horan RL, Martin I, et al. Cell differentiation by mechanical stress. Faseb J. 2002; 16:270–2. [PubMed: 11772952]

82. Germain, L.; Carrier, P.; Deschambeault, A.; Talbot, M.; Guerin, SL.; Auger, FA. Fibroblasts modulate differentiation and stratification of epithelial cells on reconstructed human cornea through the production of soluble factors. ARVO; 2004; Fort Lauderdale.

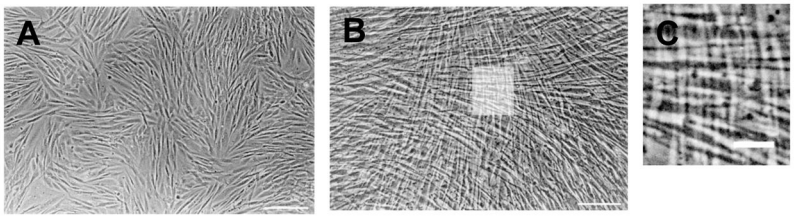

Figure 1.

Phase contrast optical micrographs of the organization of HCFs in transwell (A) At day 1, the fibroblasts cover the transwell in a monolayer of spindle-shaped cells. Bar 100 microns (B) At 1 week, the cultures have stratified to multiple layers and the cells appear to change orientation as a function of elevation above the transwell membrane. Bar = 100 microns. (C) Inset region from (B) where fibroblast orientation change appears to orthogonal. Bar = 25 microns. Images are representative of 5 experiments.

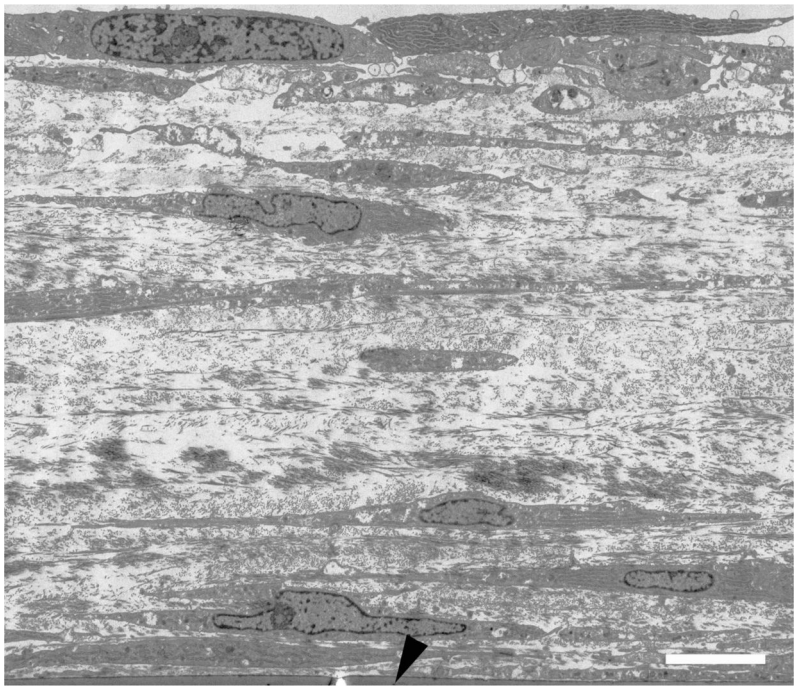

Figure 2.

Transmission electron micrograph of the organization of HCF constructs. Low magnification TEM of 4 week construct shows 32 micron thick stratified cell and ECM with confluent cellular monolayers on the top surface and adjacent to the transwell membrane (arrowhead). Bar = 5 microns. Images are representative of the 5 experiments.

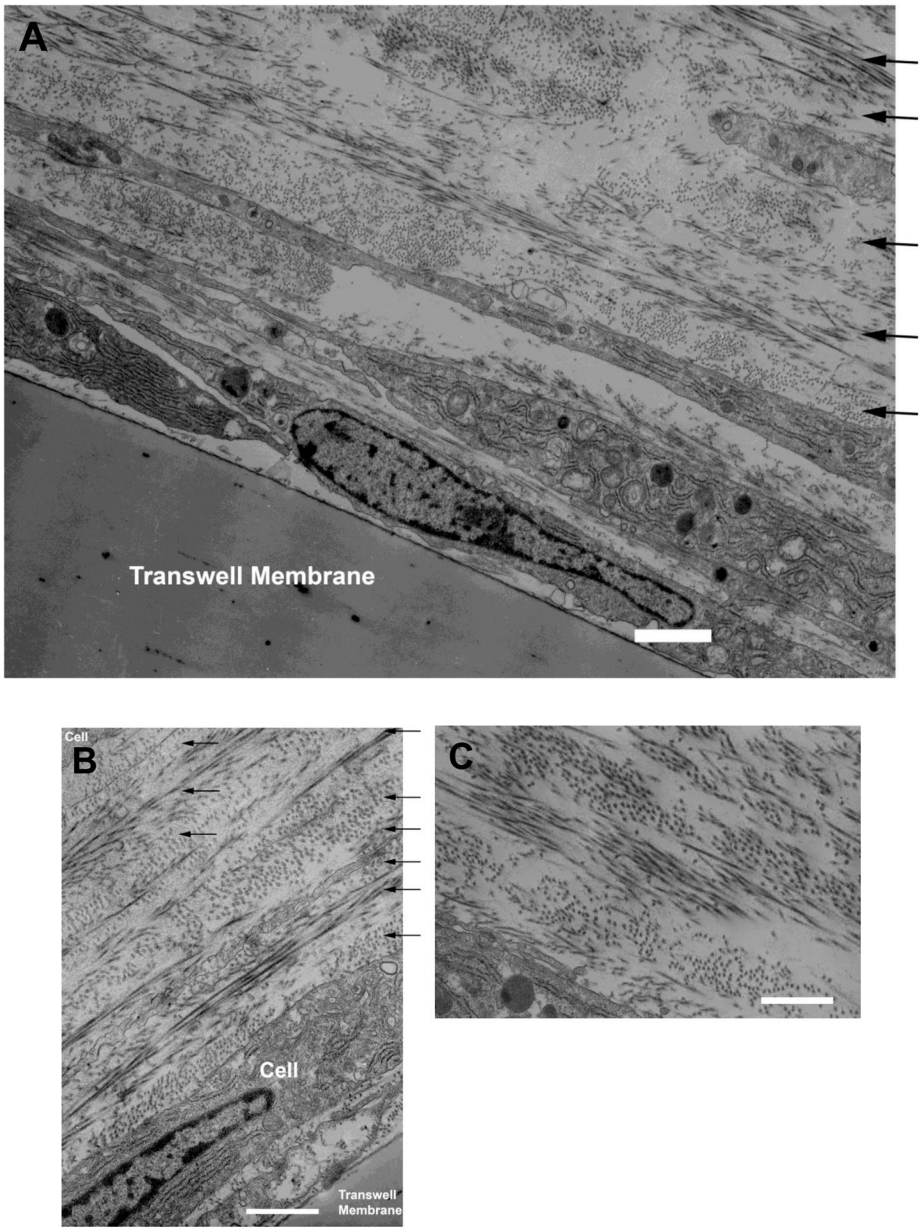

Figure 3.

TEM micrographs of lamellar-like architecture of the constructs. (A) Low magnification view of the cells and synthesized arrays of fibrils. The arrows indicate putative “lamellae” where fibril orientation appears to change direction. Of note is the fact that the “lamellae” can extend over significant (tens of microns) distances. Bar = 2 microns. (B) Higher magnification view of the organization of fibrils and their apparent change in direction within the “lamellae”. Again, arrows indicate the location of changes in fibril orientation. Bar = 2 microns. (C) High magnification view of alternating fibril arrays in the construct. Bar = 1 micron.

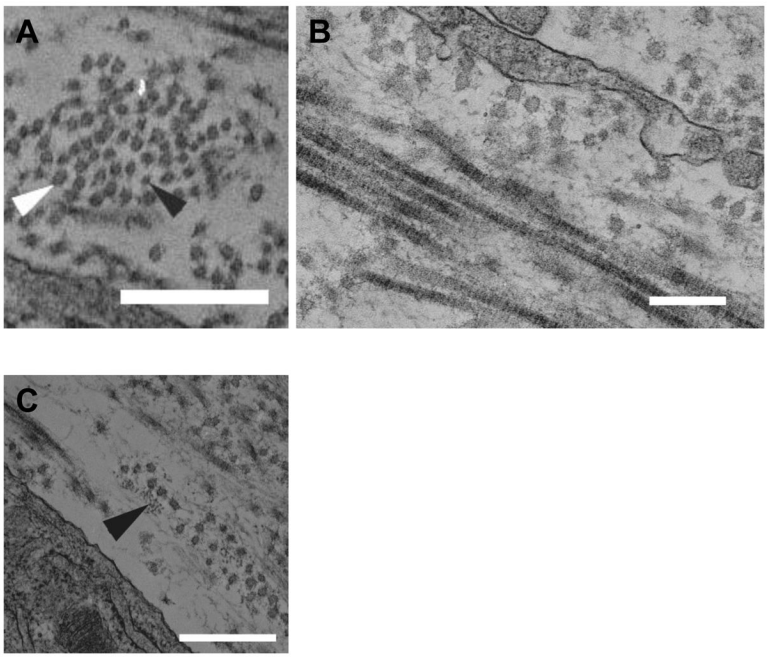

Figure 4.

Transmission electron micrographs of fibril morphology in HCF synthesized constructs. (A) Micrograph showing the diameter polydispersity (end view) of the forming fibrils. Fibril with diameter of 28 nm (black arrowhead) and fibril with diameter that is 45 nm (white arrowhead). Bar 500 nm (B) Higher magnification micrograph showing the typical banding pattern of the fibrils in the constructs. Bar = 200 nm. (C) Micrograph showing the presence of clusters of microfibrils which are similar to those found in developing mammalian stroma (arrow). Bar 500 nm.

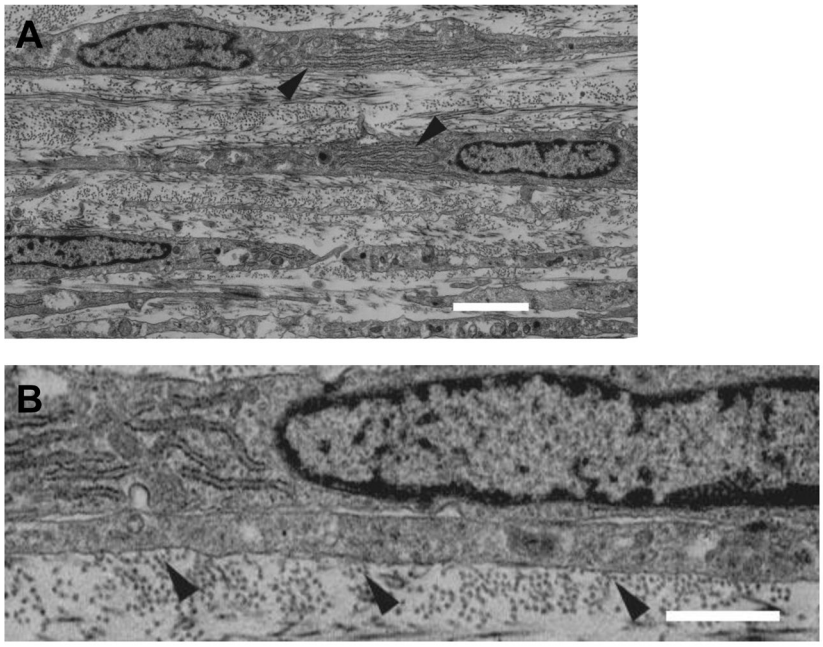

Figure 5.

Transmission electron micrographs of the architecture of the HCF synthesized constructs. (A) Dense parallel architecture of cells and cell processes between which the fibril formation is controlled. Note the presence of prominent RER (black arrowheads). Bar = 2 microns. (B) Fibrils are often found in close apposition and parallel to the surface of the cells in the construct (black arrowheads). Bar = 1 micron.

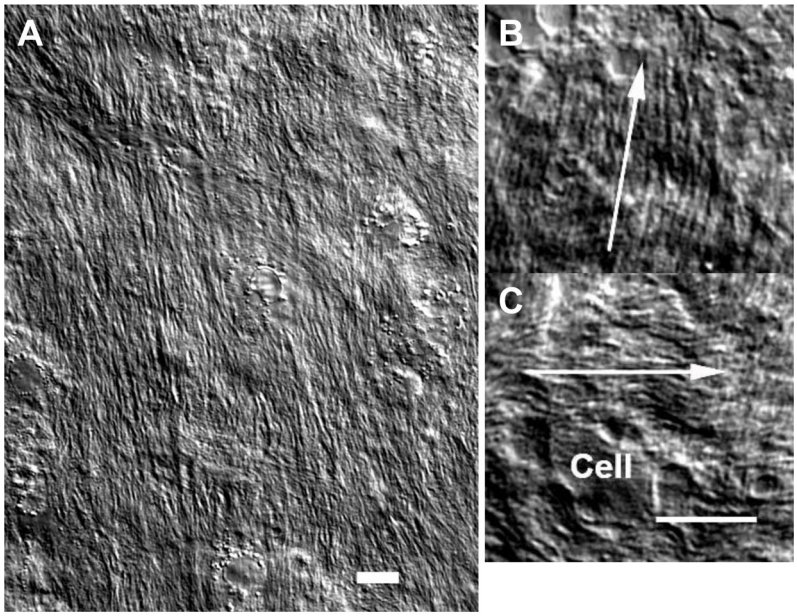

Figure 6.

Differential Interference Contrast photomicrograph of *in plane* ECM alignment. (A) Low magnification DIC imaging qualitatively demonstrates the general alignment of ECM in the middle of a 4 week construct (approximately 25 microns above the transwell membrane). Note the length over which the aligned texture of the image is consistent. Bar is 10 microns. (B) High magnification DIC showing local alignment in the direction of the arrow. (C) High magnification of same x–y location in B, but displaced 5 microns deeper into construct. The direction of ECM alignment is changing relative to the matix seen in (B). Bars = 10 microns.

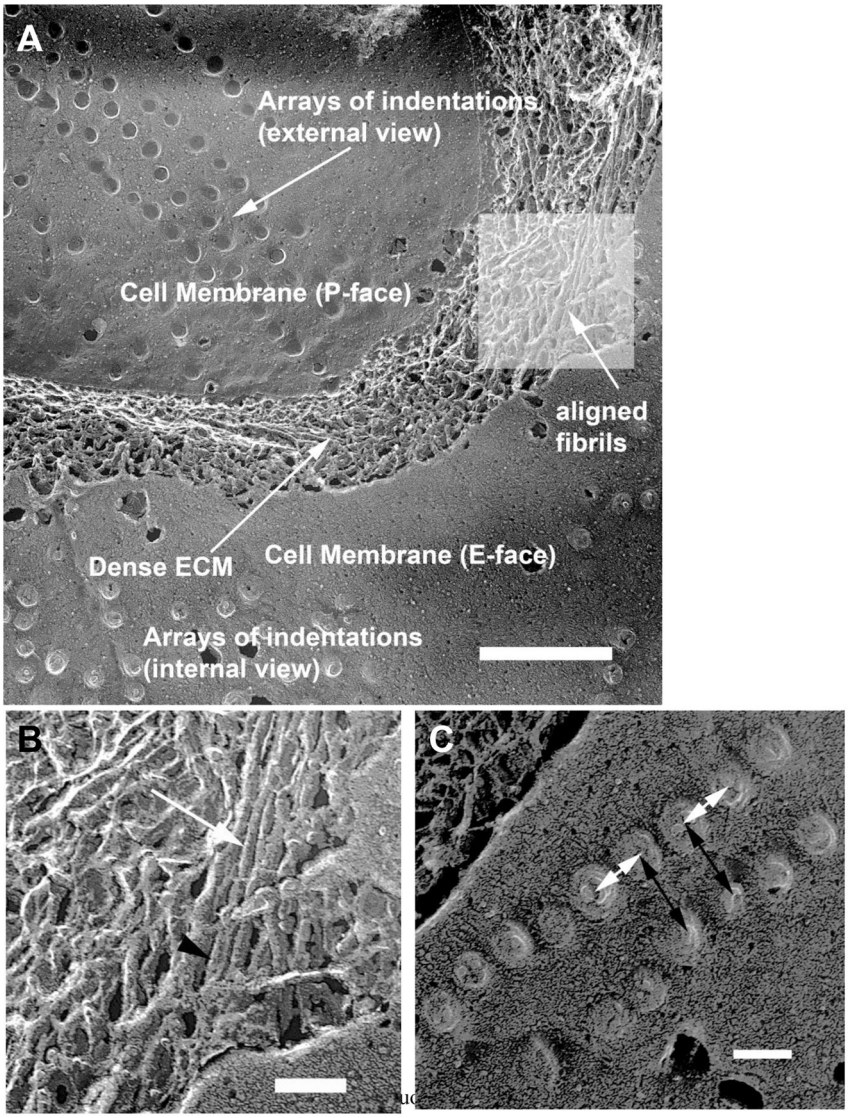

Figure 7.

Quick Freeze/Deep Etch micrograph of 5 week construct cell membranes and extracellular matrix. (A) Low magnification image of matrix between two fibroblast cells. The cell membranes display regular arrays of “indentations” of unknown function. These regular arrays of indentations on the cell membrane (P-face) and have a nominal diameter of approximately 70 nm (but vary in size). In QFDE, which involves fracturing the specimen, the indentations appear as protrusions when the cell membrane is viewed from “inside the cell” (E-face). Bar = 500 nm (B) High magnification of the matrix demonstrates that aligned fibrils are immersed in a dense, less regular ECM. The fibril diameters vary from fibril to fibril and along the axis. Bar = 100 nm. (C) Highly organized array of indentations on cell membrane (E-face). The array is closely spaced in one direction (100 nm - white arrows) and more widely spaced in the other (150+ nm - black arrows). Bar = 100 nm.

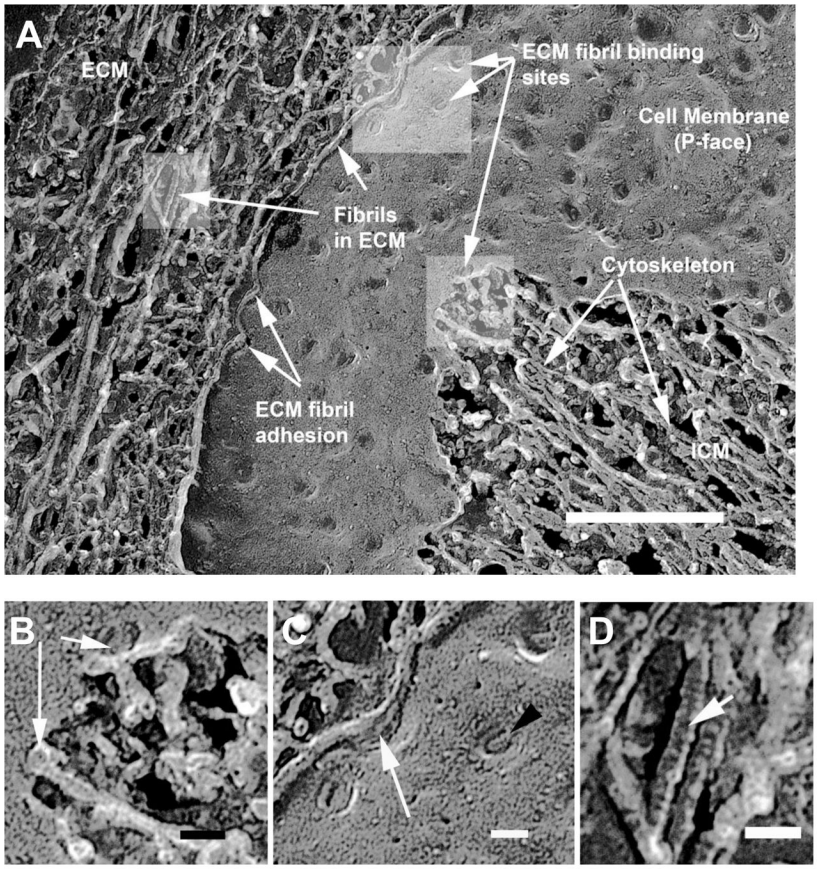

Figure 8.

QFDE micrographs of cell matrix interaction in 5 week construct. (A) Low magnification of a cell's interaction with the neighboring ECM. The image shows the intracellular matrix (ICM), the extracellular matrix (ECM), the outside of the cell membrane (P-face) and the details of ECM fibril interaction with the cellular membrane and possibly the cellular cytoskeleton. Bar = 500 nm (B) High magnification of cellular cytoskeletal interaction with the cell membrane at locations where the indentations have been disrupted by the fracture plane. The membrane appears to interact with fibrillar molecules, which span the indentation parallel to the cell surface (arrows). Bar = 50 nm. (C) High magnification image of the indentation morphology and its interaction of an ECM fibril. The indentation is spanned by a fibrillar molecule, which appears to be striated (black arrowhead). At the top of the image, an ECM fibril appears to dip into an indentation (white arrow). Bar = 50 nm (D) Striated fibrils in the matrix presumed to be outside the cell (arrow). The fibrils are about 20 nm in diameter and appear to be branched. Bar = 50 nm.

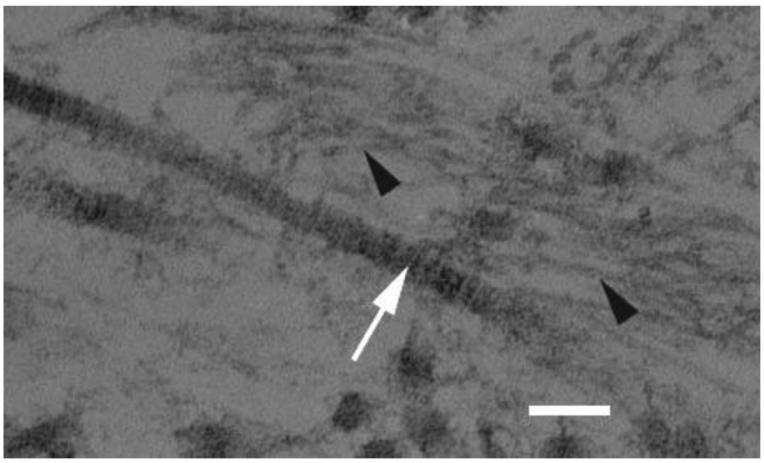

Figure 9.

Transmission electron micrograph of collagen and associated fibrillar structures. A collagen fibril (white arrow) is associated with numerous faintly stained microfibrils. These microfibrillar structures could account for the high-density of fine fibrils in the ECM detected by QFDE imaging. Bar = 100 nm. Image is representative of 5 experiments

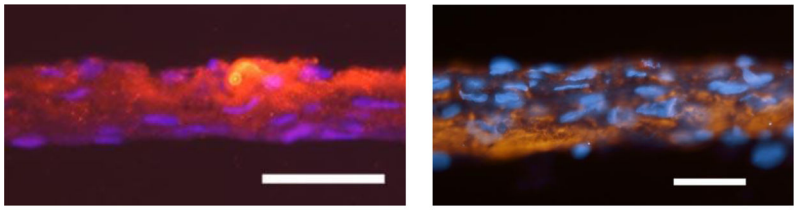

Figure 10.

Indirect immunofluorescence micrographs of collagen in HCF synthesized constructs. (A) Merged type V collagen (red) and DAPI (blue) stained construct. Some areas stained more intensely than others but type V collagen was distributed throughout the extracellular matrix. (B) Merged type VI collagen (amber) and DAPI (blue) stained construct. Type VI collagen was found throughout the tissue but appears more concentrated at the bottom of the construct. Bars = 50 microns.